



Accepted Article

Title: Beta strand mimicry: Exploring oligothiénylpyridines foldamers

Authors: Marie Jouanne; Anne Sophie Voisin-Chiret; Rémi Legay; Sébastien Coufourier; Sylvain Rault; Jana Sopkova-De Oliveira Santos

This manuscript has been accepted after peer review and the authors have elected to post their Accepted Article online prior to editing, proofing, and formal publication of the final Version of Record (VoR). This work is currently citable by using the Digital Object Identifier (DOI) given below. The VoR will be published online in Early View as soon as possible and may be different to this Accepted Article as a result of editing. Readers should obtain the VoR from the journal website shown below when it is published to ensure accuracy of information. The authors are responsible for the content of this Accepted Article.

To be cited as: Eur. J. Org. Chem. 10.1002/ejoc.201600882

Link to VoR: <http://dx.doi.org/10.1002/ejoc.201600882>

Supported by



WILEY-VCH

Beta strand mimicry: Exploring oligothiienylpyridines foldamers

Marie Jouanne, Anne Sophie Voisin-Chiret,* Rémi Legay, Sébastien Coufourier, Sylvain Rault and Jana Sopkova-de Oliveira Santos*^[a,b]

Abstract: Protein-protein interactions (PPIs) are involved in many cellular processes; consequently, the discovery of small molecules as modulators of PPIs has become an important challenge in medicinal chemistry. Structural mimetics of α -helices, β -turns or β -strands could maintain or restore biological functions and should possess biological activity. At this time, the most challenging classes of PPIs are those mediated by β -sheet interactions, which are implicated in a number of diseases. Only few β -strand mimes were published to date. This study presents the evaluation of oligothiienylpyridyl scaffolds in view of their ability for β -strand mimicry. In this study, theoretical ring twist angle predictions for these scaffolds have been validated by X-ray diffraction and molecular dynamics simulations with NMR constraints. Careful choice of substituent and heavy atom positions in the foldamer units opens the way to produce reasonably coplanar compounds mimicking β -strand side chain distribution.

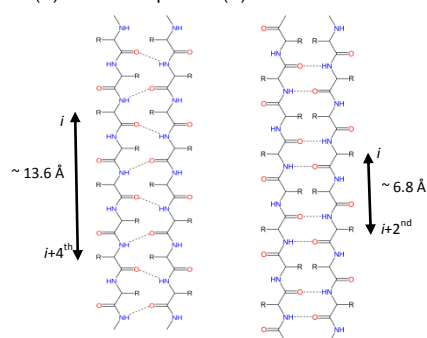
Introduction

Protein-protein interactions (PPIs) play an essential role in most biological events within a cell. The interacting macromolecules carry out cellular processes such as DNA synthesis, gene expression, signal transduction and immune responses.^[1] At the same time, aberrant PPIs are at the heart of pathological processes, such as for example cancer and neurodegenerative diseases. Atomic level structural knowledge of protein-protein complexes has shown that PPIs contain hot-spot regions on secondary structural elements, whose contribution dominates binding enthalpy.^[2] To target these interactions there is a need for nonpeptide mimics able to reproduce key distances and angular characteristics of the protein surface.^[3] Ideally, the non peptide scaffold mimic should be easily synthesized, stable under physiological conditions and allowing easy variation of the groups attached to them.

The most common type of secondary structure in proteins is the α -helix and a large body of work has already been carried out to design and synthesize α -helix mimetics.^[4] The β -sheet is the second form of regular secondary structure and it also often

mediates an interaction between proteins^[5], but β -strand mimicry remains little studied.^[6] A β -sheet consists of several β -strands, kept together by a network of hydrogen bonds between the backbone N-H and C=O groups (see Figure 1). In the fully extended β -strand, successive side chains are coplanar and point straight up, then straight down, then straight up, etc. Distances between $C_{\alpha}(i)$ and $C_{\alpha}(i+2^{nd})$ and between $C_{\alpha}(i)$ and $C_{\alpha}(i+4^{th})$ are approximately 6.8 Å and 13.6 Å respectively. To target the interaction of a β -strand in the middle of a β -sheet there is a need for nonpeptide mimetics capable to reproduce the characteristics of a β -strand.

Figure 1. Illustration of the hydrogen bonding patterns, represented by dotted lines, in a parallel (A) and an antiparallel (B) beta sheet.



To date, few β -strand mimetics have been described even though higher-level association of β -sheet has been implicated in the formation of protein aggregates and fibrils observed in many human diseases. Therefore, there is a considerable interest in developing small-molecule β -strand mimetics that can disrupt such interactions. Pioneer work of Hirschman and Smith used successfully pyrrolinone-based to design non peptide mimics of β -pleated strands and sheets.^[7] Since several years, Hamilton's group has focused on mimetics of one recognition surface of the strand (the i , $i+2^{nd}$, and $i+4^{th}$ side chain residues), using different scaffolds, such as 2,2-disubstituted-indolin-3 derived^[8], aryl-linked hydantoins^[6b] and, in a very recent work, this group was interested in aryl- and pyridyl-linked imidazolidin-2-ones^[6d], in which dipolar repulsion is a central determinant of conformation.

Our laboratory has described a methodology to design potential protein secondary structure mimes, using as structural chemical units, pyridyl, thienyl and phenyl rings: the garlanding concept.^[9] Previously, we have demonstrated the α -mimetic ability of oligopyridyl and oligophenylpyridyl scaffolds.^{[10] [11]} Today, in this article, we are interested in the capacity of oligothiienylpyridyl scaffold to mimic β -strands. In this study we have evaluated if these scaffolds are able to produce coplanar entities and if they will be able to mimic the side chain distribution of a β -strand. Studies were conducted in three steps: first, theoretical simulations were carried out in order to evaluate preferential

[a] Dr M. Jouanne, Prof. A. S. Voisin-Chiret, Dr. R. Legay, S. Coufourier, Prof. S. Rault and Prof. J. Sopkova-de Oliveira Santos Université Caen Normandie, France

[b] Dr M. Jouanne, Prof. A. S. Voisin-Chiret, Dr. R. Legay, S. Coufourier, Prof. S. Rault and Prof. J. Sopkova-de Oliveira Santos UNICAEN, CERMN - EA 4258, FR CNRS 3038 INC3M, SF 4206 ICORE bd Becquerel, F-14032 Caen, France
E-mail : jana.sopkova@unicaen.fr
Homepage : <http://cermn.unicaen.fr/>

Supporting information for this article is given via a link at the end of the document.

torsion angles between rings in thienylpyridyl systems; second, the theoretical predictions were validated by experimental data from structural studies in solution (NMR study associated with dynamic simulations) as well as in the solid state (X-ray diffraction). Finally, we assessed the ability of oligothiopyridyl substituents to mimic β -strand side chain distribution.

Results and Discussion

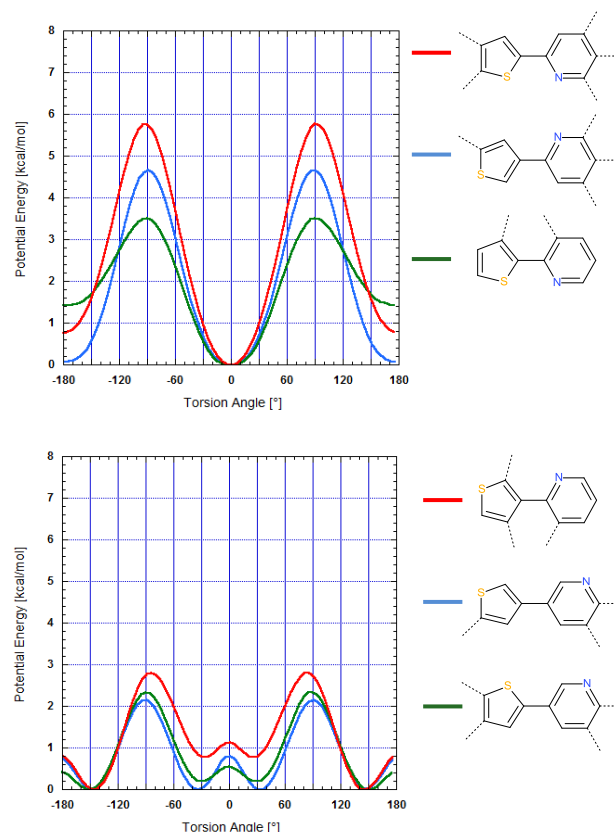
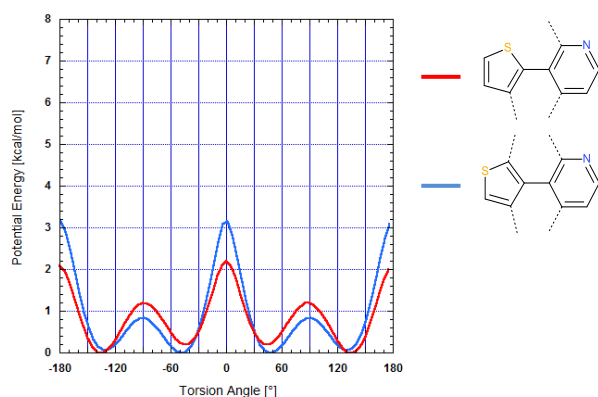
Ab initio simulation

First of all, theoretical simulations have been carried out on systems constituted of one pyridyl and one thienyl ring unsubstituted or monosubstituted with one methyl group. In the monosubstituted system, the methyl substituent was placed either on the pyridyl or the thienyl ring in different positions. The nitrogen position in the pyridyl ring and the sulfur position in the thienyl ring also varied. In total, 4 unsubstituted and 28 monosubstituted models were built, of which 16 were substituted on the pyridyl ring and 12 on the thienyl ring. Among the models, only the pyridyl ring with a nitrogen atom in the *ortho* and in *meta* positions (relative to the ring junction) are described in this paper. We do not present results concerning diaryls with nitrogen atom in the *para* position, because they are substantially similar to the *meta* position results.

For each model the internal potential energy barrier was calculated by *ab initio* simulation at (B3LYP/6-31+G(d,p)) level as a function of torsion angle between the two rings. The results for monosubstituted and unsubstituted thienylpyridine are summarized in Table 1 and Figure 2.

A detailed analysis of the results showed that the 28 monosubstituted and 4 unsubstituted models can be divided into 3 groups depending on the preferential twist angle between adjacent thienyl/pyridyl moieties and the energy barrier height associated with this twist.

Figure 2. Evolution of potential energy as a function of torsion angle between the rings in unsubstituted thienyl/pyridyl systems or monosubstituted by methyl ones.



Interestingly, our computational analysis showed that when the N and S atoms are both located in the vicinity of the junction (Table 1 and Figure 2), the rings are systematically in the coplanar arrangement (group A1 and A2) and this even in the presence of a methyl substituent in the *ortho* position relative to the ring junction (group A2). The introduction of a methyl substituent in the proximity of the junction decreased the energy barrier height by about 2 kcal/mol, but did not destabilize the coplanar arrangement. These results are in agreement with previously published theoretical calculations in which an electron deficient divalent S atom has two areas of positive electrostatic potential, a consequence of the low-lying σ^* orbitals of the C-S bond, that are available for interaction with an electron donor such as nitrogen.^[12] Consequently, the intermolecular N...S interaction was pointed out as a conformational stabilizing element introducing "N,S-*cis* locked" coplanar arrangement in biaryl systems in the analogous manner as non-covalent S...O interaction has used as conformational control element in α -helical mimetic benzothiazol-thiophene scaffold synthesized by Hamilton's group.^[13] Moreover, we observed also that the coplanar arrangement in biaryl can be achieved when N atom lies in the direct neighborhood of the junction and the other three atoms are H_{ar} (group A3). The nitrogen lone pair introduces a negative partial charge in the ring and thus a weak electrostatic interaction between N and H_{ar} occurs and plays also a role of a stabilizing element.

Table 1. Structural parameters of minimum energy conformers of methyl substituted thienylpyridine obtained from PES at B3LYP/6-31+G(d,p) level.

Group	Compound	Preferential angle between the ring planes ^a	Potential energy barrier [kcal/mol]
A	1 Preferred conformation N,S-cis-locked	Co-planar (0° - ±20°)	5.5-6
	2 Preferred conformation N,S-cis-locked	Co-planar (0° - ±30°)	3.5
	3 Preferred conformation N,S-cis-locked	Co-planar (0° - ±25°)	4.5
B	1 Preferred conformation N,S-trans-locked	30° (0° - ±50°)	2-3
	2 Preferred conformation N,S-trans-locked	30° (0° - ±50°)	2-2.5
	3 Preferred conformation N,S-trans-locked	30° (15° - ±50°)	2
C	1 Preferred conformation N,S-trans-locked	±45° (±30° - ±70°)	2-2.5
	2 Preferred conformation N,S-trans-locked	±50° (±30° - ±75°)	3-4

[a] values in brackets correspond to a 0.5 kcal/mol limit.

Nevertheless, in the latter case, the methyl substituent in the vicinity of the junction disrupts the coplanar arrangement and the ring preferential twist angle becomes about 30° with a small energy barrier ($\Delta E \sim 2$ -3 kcal/mol) (group B1). In this case, the steric repulsion between the *ortho* substituents dominates somewhat over the weak $N \cdots H_{ar}$ electrostatic interaction. A similar preferential twist angle $\sim 30^\circ$ occurred also when the four atoms in the junction vicinity were H_{ar} or when S atom and three H_{ar} were present (group B2 and B3, respectively).

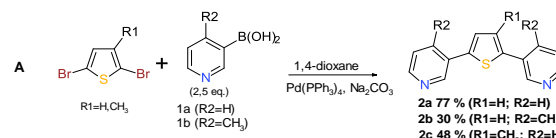
Interestingly, in biaryls of group B2 with an S atom in the junction vicinity, the introduction of a methyl group in the *ortho* position to the junction (group C1) changes the preferential twist angle from 30° to 45° but does not change the energy barrier which remains about $\Delta E \sim 2$ -2.5 kcal/mol. A similar phenomenon can be achieved also in a system with only H_{ar} in the junction vicinity (group B3); the introduction of a methyl substituent increased the preferential ring twist angle to 50° (group C2). In these systems, the bulky methyl group in the *ortho* position to the junction introduces a more important steric repulsion and so the potential energy barrier increases from 2 to 4 kcal/mol.

Finally the adjacent thienyl/pyridyl rings are balanced by four competing factors; (i) the interaction between the electron-donating N atom and the acceptor S atom,^[12] (ii) electrostatic interaction due to the presence of nitrogen, (iii) a symmetric interaction between π orbitals of the aromatic rings, (iv) a steric repulsion between overlapping *ortho* hydrogen atoms and substituents.^[14] Our simulation results suggested that we can introduce a coplanar or near coplanar arrangement in oligothiopyridines in several ways contrary to the biphenyl for which the co-planar arrangement has never been achieved. Despite the fact that the introduction of substituent in *ortho* in oligothiopyridines deviates the adjacent rings from coplanar arrangement, the energy barriers related to the twist angles remain small (< 4 kcal/mol) allowing flexibility in the thienylpyridyl scaffolds. Contrariwise the *ortho* substituents in biphenyl have increased significantly the energy barrier (from 4 kcal/mol to 12 kcal/mol.^[9e, 15] So, the thienylpyridyl scaffolds will more easily reach coplanar arrangements with smaller energies penalties in comparison with oligophenyl scaffolds and is therefore more suitable for beta strand mimicry.

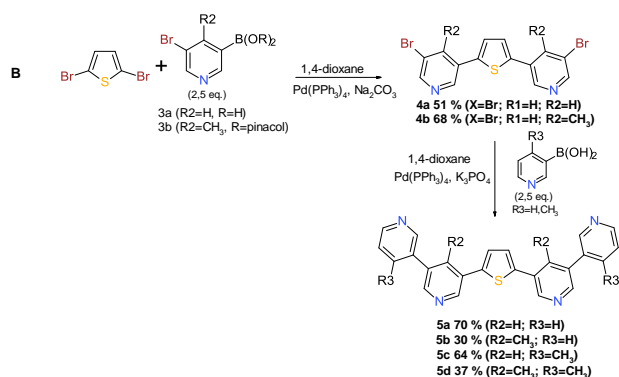
Compound Synthesis

In order to validate our theoretical predictions, calculated for simple two-unit systems, various thienylpyridines with three or five diversely substituted units were synthesized (Table 2). Our laboratory is specialized in the preparation and use of boronic species^[16] and in the study of their ability to be good cross-coupling partners.^[9f, 17] With this expertise, oligothiopyridines using Suzuki-Miyaura cross-coupling reaction were synthesized. Three unit compounds **2a-c** (scheme 1A) and **4a-b** (scheme 1B) were prepared from a Suzuki-Miyaura cross-coupling reaction between a 2,5-dibromothiophene and two equivalents of a pyridylboronic acid. Under to the same conditions, starting from dibromothiopyridines **4a-b**, five unit compounds **5a-d** (scheme 1B) have been obtained. This last synthesis procedure allows the preparation of symmetrical molecules only. To evaluate more finely the impact of sulfur/nitrogen interactions on the overall molecule conformation, dissymmetrical three unit compounds (**8a-b**) were also synthesized using a sequence Suzuki-Miyaura reaction - bromination - Suzuki-Miyaura reaction (scheme 2).

Scheme 1A. A mixture of pyridylboronic acid **1a** or **1b** (2.5 equiv), 2,5-dibromothiophene or 2,5-dibromo-3-methylthiophene (1.0 equiv), tetrakis(triphenylphosphine) palladium (10 mol %), and aqueous Na_2CO_3 (5 equiv) in 1,4-dioxane was heated to reflux for 20h until the complete consumption of dibromothiophene (TLC). Crude products were purified by silica gel column chromatography to give 3-[5-(3-pyridyl)-2-thienyl]pyridine **2a**, 4-methyl-3-[5-(4-methyl-3-pyridyl)-2-thienyl]pyridine **2b** and 3-[3-methyl-5-(3-pyridyl)-2-thienyl]pyridine **2c** with 77%, 30% and 48% yield, respectively.



Scheme 1B. A mixture of bromopyridylboronic acid **3a** or pinacol ester **3b** (2.5 equiv), 2,5-dibromothiophene (1.0 equiv), tetrakis(triphenylphosphine) palladium (10 mol %), and aqueous Na₂CO₃ (5 equiv) in 1,4-dioxane was heated to reflux for 20h until the complete consumption of dibromothiophene (TLC). Crude products were purified by silica gel column chromatography to give 3-bromo-5-[5-(5-bromo-3-pyridyl)-2-thienyl]pyridine **4a** and 3-bromo-5-[5-(5-bromo-4-methyl-3-pyridyl)-2-thienyl]-4-methyl-pyridine **4b** with 51% and 68% yield, respectively. Then **4a** or **4b** (1.0 equiv) was dissolved in 1,4-dioxane and 3-pyridylboronic acid or 4-methyl-3-pyridylboronic acid (2.5 equiv), tetrakis(triphenylphosphine) palladium (10 mol %), and aqueous K₃PO₄ (5 equiv) were added. The reaction mixture was heated to reflux for 20h until the complete consumption of dibromopyridylthienylpyridine (TLC). Crude products were purified by silica gel column chromatography to give 3-(3-pyridyl)-5-[5-(3-pyridyl)-3-pyridyl]-2-thienylpyridine **5a**, 4-methyl-3-[5-[4-methyl-5-(3-pyridyl)-3-pyridyl]-2-thienyl]-5-(3-pyridyl)pyridine **5b**, 3-(4-methyl-3-pyridyl)-5-[5-[5-(4-methyl-3-pyridyl)-3-pyridyl]-2-thienyl]pyridine **5c** and 4-methyl-3-[5-[4-methyl-5-(4-methyl-3-pyridyl)-3-pyridyl]-2-thienyl]-5-(4-methyl-3-pyridyl)pyridine **5d** with 70%, 30%, 64% and 37% yield, respectively.



Scheme 2. 2-thienylboronic acid (1.0 equiv), 2-bromopyridine or 2-bromo-3-methylpyridine (1.0 equiv), tetrakis(triphenylphosphine) palladium (5 mol %), and aqueous Na₂CO₃ (2.5 equiv) were added in 1,4-dioxane and the mixture reaction was heated to reflux for 12h until the complete consumption of bromopyridine (TLC) to obtain 2-(2-thienyl)pyridine **6a** (67%) and 3-methyl-2-(2-thienyl)pyridine **6b** (78%) after purification by silica gel column chromatography. Then, to a stirred solution of **6a** or **6b** in a 50/50 (v/v) mixture of dichloromethane and glacial acetic acid was added N-bromosuccinimide (NBS) (1.1 equiv). The resulting solution was stirred at 40°C for 3-12h and the crude product was subjected to column chromatography to give desired bromothiopyridine **7a** (50%) and **7b** (91%). Finally, **7a** (1.0 equiv) was dissolved in 1,4-dioxane and 3-pyridylboronic acid (1.2 equiv), tetrakis(triphenylphosphine) palladium (5 mol %), and aqueous K₃PO₄ (2.5 equiv) were added. The reaction mixture was heated to reflux for 20h until the complete consumption of **7a** (TLC). Crude product was purified by silica gel column chromatography to give 2-[5-(3-pyridyl)-2-thienyl]pyridine **8a** with 60% yield. The same procedure was conducted with **7b** and 4-methyl-3-pyridylboronic acid to obtain 3-methyl-2-[5-(4-methyl-3-pyridyl)-2-thienyl]pyridine **8b** with 50% yield.

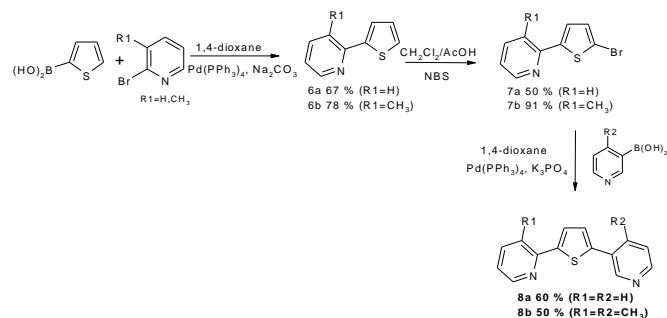


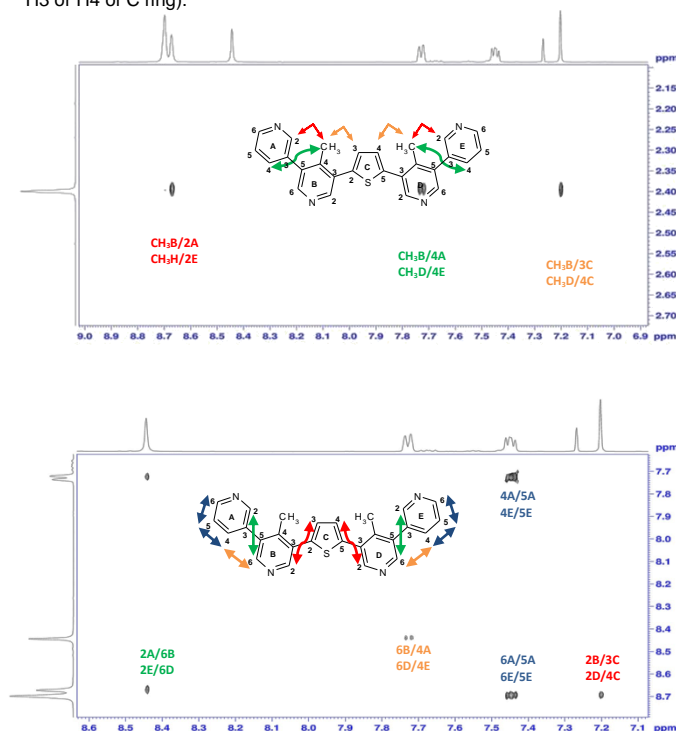
Table 2. Synthesized thienylpyridines for this study.

Name	Molecular diagram
2a	
2b	
2c	
8b	
8a	
5a	
5b	
5c	
5d	

NMR

First, an NMR structural study was carried out with the aim of analyzing 3D structures of synthesized compounds in solution. In the first step of this study, a complete assignment of all protons and carbons was realized using conventional 1D and 2D experiments: DEPT135, COSY (¹H-¹H), HSQC (¹H-¹³C), and HMBC (¹H-¹³C). The proton and carbon chemical shift values and ¹H-¹H coupling constants of **5b** are reported in Table 3 (NMR data for all studied compounds are available in the Supporting Information Table S1). In a second step, the NOESY (¹H-¹H) experiment was used to access compound conformations in solution.^[18] Indeed a correlation peak between two protons observed in the 2D spectrum indicates that these two nuclei are close through space (strong NOE intensities: distance between protons ≤ 2.5 Å; medium NOE intensities: distance between protons ≤ 3.7 Å; weak NOE intensities: distance between protons ≤ 5.0 Å). For example in the NOESY spectrum of **5b**, Figure 3A depicts a spatial proximity between methyl groups and some protons of adjacent rings and Figure 3B gives measured intracycle NOE correlations between neighboring protons in the aromatics region.

Figure 3. NOESY spectrum of thienylpyridine **5b**: (A) correlations with methyl groups; a spatial proximity between methyl group protons of neighboring pyridine rings A/E (H2, H4) and protons of the central thiophene ring C (H3, H4). (B) measured intracycle NOE correlations between neighboring protons in the aromatics area: first, correlations between neighboring hydrogens of the same ring (H4, H5 and H6 in A/E rings) and second, intercycle spatial proximity correlations between protons located on each side of the ring junctions (H6 of B/D rings with H2 and H4 of rings A/E, H2 of B/D rings with H3 or H4 of C ring).



Furthermore, NOESY experiments allow a quantitative estimation of internuclear distances in small to intermediate size molecules.^[19] NOE correlation intensities (I) depend on distances between two protons as follows: $I = k/r^6$. The constant k is estimated from the integration of a NOE correlation spot between two intracycle protons separated by a distance r , known or determined by X-ray crystallography and a priori independent of molecule conformation. We performed calculations using several different references whenever it was possible. Integrating the correlation spot volumes and using the relation ($I = k/r^6$), an estimate of the corresponding distances with an error margin of 20 to 25% was obtained (due to spin diffusion, other relaxation mechanisms, complicated modes of motion, affecting NOEs intensities). The estimated distances from NMR spectra for **5b** are given in Table 3 and those for all studied compounds are available in the Supporting Information (Table S1).

Then molecular dynamic simulations at 300 K were carried out with the application of ^1H - ^1H distance constraints determined from the NMR study (NMR constraints). Starting from initial coordinates built using the Discovery Studio software^[20], these simulations led to NMR thienylpyridyl 3D structures. In simulations we used only the force field derived by the Discovery Studio and experimental NMR constraints without the

introduction of supplementary dihedral force field parameters based on our quantum mechanics simulations. For each derivative the 10 lowest energy conformers (as shown in Table S2 of SI) were retained for subsequent analysis from 50 ns simulations.

Table 3. $^1\text{H}/^{13}\text{C}$ NMR data for thienylpyridine **5b** and estimated distances from NMR spectra and the X-ray structure.

		$^1\text{H}/^{13}\text{C}$		^{13}C	
		δ (ppm)	J (Hz)		δ (ppm)
Rings A / E	H2	8.67	d (1.5)	C2	150.0
	H3	-	-	C3	133.7
	H4	7.73	dt (7.8, 1.7)	C4	136.8
	H5	7.45	dd (7.8, 4.9)	C5	123.4
	H6	8.70-8.69	m	C6	149.2
Rings B / D	H2	8.70-8.69	m	C2	150.1
	H3	-	-	C3	130.7
	H4	-	-	C4	143.2
	H5	-	-	C5	134.8
	H6	8.44	s	C6	149.5
Ring C	CH ₃	2.40	s	CH ₃	18.3
	H2 / H5	-	-	C2 / C5	139.9
	H3 / H4	7.20	s	C3 / C4	128.4

NOE	X-ray distance (Å)	Estimated NOE distance (Å)
CH ₃ B/2A ; CH ₃ D/2E	2.901	3.3±0.3
CH ₃ B/4A ; CH ₃ D/4E	4.850	3.2±0.3
CH ₃ B/3C ; CH ₃ D/4C	2.880	3.2±0.3
3C/2B ; 4C/2D	4.430	3.0±0.3
*5A/6A ; 5E/6E	2.280	2.5±0.2
*5A/4A ; 5E/4E	2.359	2.2±0.2
4A/6B ; 4E/6D	2.422	3.2±0.3
6B/2A ; 6D/2E	4.187	3.2±0.3

* notes the distance used as reference for NOE estimation


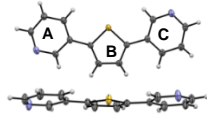
The ten most stable NMR conformers of **2a**, **2b**, **2c**, **8a** and **8b** generated, which are three unit scaffolds, were close each other in terms of absolute values of ring torsions. The observed differences among NMR conformers in one compound were related to a rotation of the same angle but in the opposite sense to one or two scaffold outside rings. This observation is in agreement with the theoretical simulations that have predicted that all thienylpyridines can rotate left and right with equal probability. For **2b**, **2c**, **8a** and **8b**, the ten conformers could be divided into two groups which differ from each other only by the torsion of one outside ring (Figure 3). In **2a** both outside rings, A and C, turned, but nonetheless its ten NMR conformers cluster also in 2 groups, because the A and C rings turned on the opposite sense at the same time.

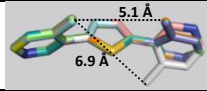
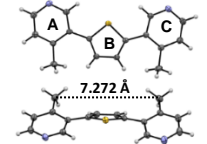
The NMR structures of three-unit scaffolds generated were compared to the theoretical predictions (Figure 4). For each compound, the twist angle values of NMR data presented in Figure 4 correspond to the average calculated from absolute twist angle values of the ten conformers (see Table S2 in Supporting Information). An overview of these results indicated that three-unit 3D NMR structures fall fully into predicted twist angles interval from the theoretical study. Nevertheless, the predicted N,S-*cis* locked conformation from the simulation of nitrogen and sulfur situated in the junction proximity was not fully confirmed by NMR structures. The N,S-*cis* conformation was observed in **8a** but it was not observed in **8b**.

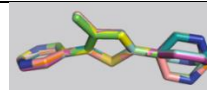
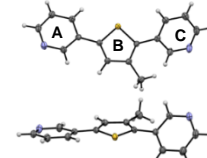
In the three-unit compounds with two substituents, **2b** and **8b**, methyl groups were situated in one cluster of conformers on the same side of the molecule, while in the other cluster they were positioned on the opposite side. The distance between methyl groups in conformers with substituents on the same side was about 5.1 Å in **2b** and 6 Å in **8b**, somewhat closer to the target one between *i*, *i*+2nd side chains of a β -strand (6.8 Å).

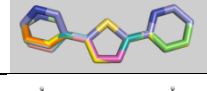
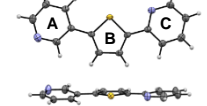
For all five-unit scaffolds studied, the ten NMR conformers generated were very close to each other and the rings have remained in the same direction. The observed twist angles in the NMR structures coincide with the predicted twist angle intervals with the exception of the B ring–C ring and C ring–D ring twist angles in **5b** and in **5d** (Figure 4). These four torsion angles match with the same motif, 4-methyl-3-(2-thienyl)pyridine, which in both compounds lie inside the five unit scaffold. In **5b**, the B ring–C ring and C ring–D ring twist angles were slightly out of the predicted value interval and deviations were small, about 4°. Moreover, these deviations introduce only small energy penalties ($\Delta E_{\text{penalty}} \sim 0.5$ kcal/mol, Figure 2). In **5d**, the deviation is more significant (close to 20°), but it does not introduce any greater energy penalty ($\Delta E_{\text{penalty}} \sim 0.6$ kcal/mol, Figure 2). The affected twist angle in these two compounds is one with a very small energy barrier that does not exceed overall 2.5 kcal/mol, consequently a wide deviation from optimal twist angle value introduces only a small energy penalty.

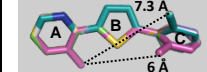
Figure 4. Stick presentations of NMR structures and ORTEP views of the crystal structures with twist angle values of 2a-c, 5a-d and 8a-b. In ORTEP diagrams, the displacement ellipsoids are drawn at the 50% probability level and H atoms are shown as small spheres of arbitrary radii.

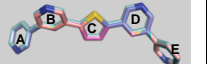
2a		\angle Ring A–Ring B	\angle Ring B–Ring C
Prediction		0° - ±50° ($\Delta E \sim 2.5$ kcal/mol)	0° - ±50° ($\Delta E \sim 2.5$ kcal/mol)
NMR data		28.1±0.1	28.1±0.1
X-ray data		6.92	-4.62
Conf. 1		6.92	-4.62
Conf. 2		-6.92	+4.62

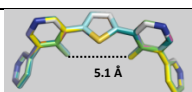
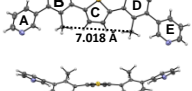
2b		\angle Ring A–Ring B	\angle Ring B–Ring C
Prediction		±30° - ±70° ($\Delta E \sim 2.5$ kcal/mol)	±30° - ±70° ($\Delta E \sim 2.5$ kcal/mol)
NMR data		66.5±0.1	66.6±0.3
X-ray data		-29.28	+33.01
Conf. 1		-29.28	+33.01
Conf. 2		+29.28	-33.01

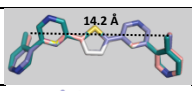
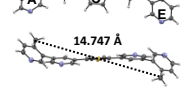
2c		\angle Ring A–Ring B	\angle Ring B–Ring C
Prediction		0° - ±50° ($\Delta E \sim 2.5$ kcal/mol)	±30° - ±70° ($\Delta E \sim 2.5$ kcal/mol)
NMR data		32.8±0.9	61±2
X-ray data		+7.38	+44.71
Conf. 1		+7.38	+44.71
Conf. 2		-7.39	+44.71

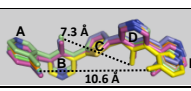
8a		\angle Ring A–Ring B	\angle Ring B–Ring C
Prediction		0° - ±50° ($\Delta E \sim 2.5$ kcal/mol)	±0° - ±20° ($\Delta E \sim 5.5-6$ kcal/mol)
NMR data		31.85±0.03	0.5±0.2
X-ray data		-10.10	+2.73
Conf. 1		-10.10	+2.73
Conf. 2		+10.11	-2.73

8b		\angle Ring A–Ring B	\angle Ring B–Ring C
Prediction		0° - ±30° ($\Delta E \sim 3.5$ kcal/mol)	±30° - ±70° ($\Delta E \sim 2.5$ kcal/mol)
NMR data		22.9±0.5	59±1

5a		\angle Ring A–Ring B	\angle Ring B–Ring C	\angle Ring C–Ring D	\angle Ring D–Ring E
Prediction		±35° - ±70° ($\Delta E \sim 3$ kcal/mol)	0° - ±50° ($\Delta E \sim 2.5$ kcal/mol)	0° - ±50° ($\Delta E \sim 2.5$ kcal/mol)	±35° - ±70° ($\Delta E \sim 3$ kcal/mol)
NMR data		69.27±0.02	24.9±0.4	24.9±0.5	69.3±0.02

5b		∠ Ring A- Ring B	∠ Ring B- Ring C	∠ Ring C- Ring D	∠ Ring D- Ring E
Prediction		±55° - ±90° (ΔE-9.5 kcal/mol)	±30° - ±70° (ΔE-2-2.5 kcal/mol)	±30° - ±70° (ΔE-2-2.5 kcal/mol)	±55° - ±90° (ΔE-9.5 kcal/mol)
NMR data		88.77±0.02	73.98±0.01	73.96±0.02	88.78±0.02
X-ray data					
		+46.70	-36.60	+36.60	-46.76
		+46.70	+36.60	-36.60	+46.76

5c		∠ Ring A- Ring B	∠ Ring B- Ring C	∠ Ring C- Ring D	∠ Ring D- Ring E
Prediction		±55° - ±90° (ΔE-9.5 kcal/mol)	0° - ±50° (ΔE-2-2.5 kcal/mol)	0° - ±50° (ΔE-2-2.5 kcal/mol)	±55° - ±90° (ΔE-9.5 kcal/mol)
NMR data		77.96±0.02	26.0±0.4	25.5±0.4	65.28±0.02
X-ray data					
		+54.22	-13.00	-13.00	+54.22
		-54.22	+13.00	+13.00	-54.22

5d		∠ Ring A- Ring B	∠ Ring B- Ring C	∠ Ring C- Ring D	∠ Ring D- Ring E
Prediction		±60° - ±90° (ΔE-25 kcal/mol)	±30° - ±70° (ΔE-2-2.5 kcal/mol)	±30° - ±70° (ΔE-2-2.5 kcal/mol)	±60° - ±90° (ΔE-25 kcal/mol)
NMR data		84.4±0.1	88±3	83±5	84.2±0.1

For the five-unit compounds, we observed that in compounds with two substituents, **5b** and **5c**, methyl groups were situated on the same side of the compounds. While in the compound with four substituents (**5d**), methyl groups on the inside rings pointed to the opposite side of compound but methyl groups on the outside rings were located once more on the same side. The distance between the methyl substituents on outside rings in **5c** and in **5d** was about 14.2 Å and 10.5 Å, respectively, and the methyl distance on inside rings in **5b** was about 5.1 Å. The observed methyl interdistances in the NMR structures are somewhat further from the target for β -strand mimes, 6.8 and 13.6 Å. However, the selected NMR structures reflect only one part of the conformational space, for example for compound **5b** ten structures in energy range of 61.2975 to 61.2976 kcal/mol (Table S2 in Supporting Information) were selected from 10000 in energy range of 61.2975 to 67.8870 kcal/mol generated in molecular dynamic simulation. For more information on the ability of thienylpyridyl scaffold to mimic a β -strand, an X-ray diffraction analysis in solid state was carried out.

X-ray structures

Suitable crystals for X-ray diffraction study were obtained for 6 derivatives from the 9 studied by NMR analysis and their 3D

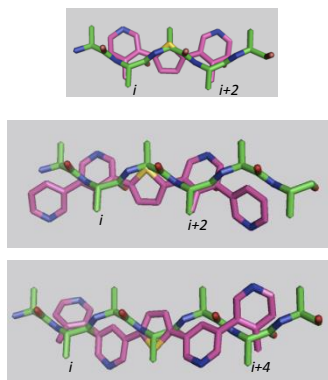
structures have been solved (Figure 4). Crystal observation under microscope showed for each derivative only one kind of crystals (needles) and there is probably no polymorphism. Therefore, the X-ray structures can be considered as representative. For each crystallized compound, the crystal space group contains a symmetric center and consequently two axial atropoisomers are present each time in the crystal with the opposite side ring rotation.

Globally, deviations between rings observed in the X-ray structures were systematically of lesser magnitude compared to those observed in the NMR analysis. Consequently, crystal structures of **2a** and **8a**, were planar and those of **2b**, **2c**, **5b** and **5c** were quite coplanar. The predicted values from the *ab initio* simulations on thienylpyridine systems were in good agreement with the observed twist angles in the X-ray structures, even for **5b** for which we observed a small deviation from the predicted value during NMR analysis. The B ring-C ring and C ring-D ring crystal twist angles were of about 37° instead of 74° observed in NMR structures. Therefore the global X-ray structure of **5b** is more planar than the NMR one. Unfortunately, we have not obtained suitable crystals for X-ray diffraction for **5d**, but we can assume that the **5d** twist angle values will be smaller as was observed for all studied compounds.

Furthermore, the simulations have suggested that for the compounds with a sulfur and nitrogen atom in the proximity of the junction, intermolecular N...S interactions should lead to a "N,S-*cis* locked" coplanar arrangement. Indeed in the crystal structure of **8a**, as well as for 5-[5-(2-pyridyl)-2-thienyl]pyrimidine (unpublished data) with sulfur and nitrogen atoms in the junction vicinity, N,S-*cis* lock was observed and rings were coplanar. Unfortunately, we did not obtain crystals of **8b** for which the NMR structure analysis proposed a N,S-*trans* arrangement contrary to our prediction.

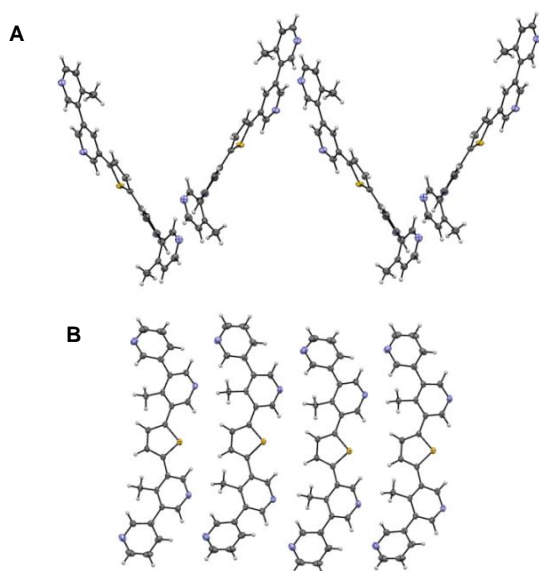
In all X-ray structures of compounds with two methyl substituents (**2b**, **5b**, **5c**), methyl groups were positioned on the same side and their interdistances were longer to those observed in NMR structures related to greater planarity of compounds in crystal. Consequently, the observed methyl interdistances in crystal structures were much closer to those desired for β -strand mimes (see Figure 1 and Figure 4). In the three-unit scaffold **2b**, methyl groups were at a distance of 7.272 Å and in the five-unit scaffold **5b** at a distance of 7.018 Å. Even if, in the structure of **5c**, methylpyridines located at both extremities deviate somewhat from coplanar arrangement (the ring twist angle related with the end pyridine was about 54°), the whole compound remained relatively coplanar and the distance between methyl groups was about 14.747 Å. In view of these results, we can expected that compounds **2b** and **5b** could be potential mimes for the *i, i+2nd* side chains of a β -strand and **5c** could mime the *i, i+4th* β -strand side chains. Alignments of X-ray structures of these three compounds with the ideal polyalanine β -strand have demonstrated that methyl substituents are projected close to the desired positions, even for the less planar compound **5c** (Figure 5).

Figure 5. Superposition of a polyalanyl β -strand (in green) and X-ray structure (in purple) of thienylpyridines with two or four substituents.



Furthermore, in the crystal packing of **5b** and **5c**, weak electrostatic interactions occurred between the pyridine N atoms and aromatic H_{ar} of a neighboring molecule. These interactions lead to the formation of a complex arrangement in the crystal. In the **5c** crystal, the N atom of an outside pyridine interacted with H_{ar} of the neighboring molecule inside pyridine, the nitrogen atoms of each outside pyridine lying in a different neighboring molecule. Consequently, the **5c** forms a “zigzag” chain across the entire crystal (Figure 6). In **5b** the nitrogen of both inside pyridines established weak electrostatic interactions with an outside pyridine H_{ar} and with the methyl group of a neighboring compound. Moreover, in **5b** packing, the two inside N atoms related to the same neighboring molecule. Therefore, the **5b** compound established a sheet-like arrangement in the crystals (Figure 6). The H_{ar} committed in these weak electrostatic interactions within crystals were systematically those situated at *ortho* of the N atom.

Figure 6. A general view of the crystal packing of **5c** (A) and **5b** (B).



Conclusions

We have demonstrated that we can obtain a coplanar arrangement in thienylpyridyl systems in several different ways. The presence of a nitrogen and sulfur atom in the junction vicinity introduces a coplanar arrangement (regardless of the substituent position) as well as the presence on nitrogen in the *non-ortho* substituted systems. The introduction of an *ortho* substituent in a system with nitrogen in the junction vicinity deviates somewhat the two rings ($\pm 30^\circ$), but the system can achieve the same close coplanar arrangement since the energy barrier corresponding to the 0° twist angle is very low in these systems, about of 0.5 kcal/mol. The same behavior was observed in a *non-ortho* substituted biaryl with only a sulfur in the junction vicinity. The X-ray structures showed that the compounds have a tendency to generally adopt a nearly coplanar conformation so that the positions of methyl substituents coincide well with those of *i*, *i*+2nd or *i*, *i*+4th β -strand side chains. Interestingly, the crystal structure analysis showed that **5b** is itself able to form a sheet-like structure. Therefore, the thienylpyridine scaffold opens the way to produce coplanar compounds mimicking β -strand side chain distributions.

Experimental Section

Conformational Analysis.

3D models for thienylpyridines as a function of the pyridyl nitrogen, thienyl sulfur and methyl position were built using the Discovery Studio software.^[20] This corresponds to 28 thienylpyridyl models substituted with one methyl group and 4 unsubstituted models. The Cartesian coordinates of each model were used as input for the *ab initio* simulation. All *ab initio* calculations reported in the present study were carried out using the Gaussian 03 software.^[21] Potential energy scan (PES) studies of all thienylpyridines consisted of a (-180° , $+180^\circ$) geometry optimization with the specified coordinate freezing and a 5° increment in order to obtain the internal energy barrier to rotation at the B3LYP/6-31+G(d,p) level.

Compounds synthesis

General Procedure for Suzuki-Miyaura Cross-Coupling used for compound synthesis is presented in Schemes 1 and 2. Commercial reagents were used without further purification. Chromatography was carried out on a column using flash silica gel 60 Merck (0.063-0.200 mm) as the stationary phase. Flash chromatographies were performed with a Biotage Isolera One flash chromatography. The eluting solvent, indicated for each purification, was determined by thin layer chromatography (TLC) performed on 0.2 mm precoated plates of silica gel 60F-264 (Merck) and spots were visualized using an ultraviolet-light lamp. Melting points (Mp) were determined using a Köfeler heating bench. Infrared (IR) spectra were recorded on a Perkin Elmer FT-IR spectrophotometer. The band positions are given in reciprocal centimeters (cm^{-1}). Mass data were recorded on a liquid chromatography-mass spectrometer Waters SQD in ESI+ or ESI- mode. High resolution mass spectra were performed at 70

eV by electronic impact (HRMS/EI) or by positive or negative electrospray (HRMS/ESI).

NMR Measurements

All NMR experiments were carried out using a Bruker AVANCE III 500 spectrometer equipped with a 5 mm BBFO $\{^1\text{H}, ^{13}\text{C}\}$ including shielded z-gradients. Solutions in concentration range of 20–30 mg·mL⁻¹ in CDCl₃ were used. Experiments were carried out at 500 MHz for ^1H and 125 MHz for ^{13}C . ^1H and ^{13}C chemical shifts are expressed in parts per million (ppm) and referenced according to the CDCl₃ solvent signal used as a secondary internal reference (^1H , $\delta=7.26$ ppm; ^{13}C , $\delta=77$ ppm, with respect to TMS, 0 ppm). The 1D and 2D NMR spectra were measured at 295 K. Complete assignment of all protons and carbons was carried out using conventional 2D experiments: COSY (^1H – ^1H), HSQC (^1H – ^{13}C), and HMBC (^1H – ^{13}C). For all 2D spectra, a total of 4096 points in F2 and 512 experiments in F1 were recorded. For the HMBC experiment, an evolution delay of 65 ms was chosen in such a way that correlations involving long-range J coupling around 10 Hz could be observed. To observe through space correlations, NOESY (^1H – ^1H) experiments were performed using mixing times of 1.5 s. Processing and analysis of the NMR spectra was performed with the Topspin 3.2 software from Bruker.

X-ray diffraction.

Single crystal X-ray analysis was carried out at 150 K using graphite-monochromatized Mo K α radiation on a Bruker-Nonius Kappa II diffractometer equipped with a CCD area detector. The crystal structure was solved by direct methods using the SHELX97 package^[22] and refined using SHELXL^[23]. The refinement was based on F^2 for all reflections, and all non-hydrogen atoms were refined anisotropically. Hydrogen atom positions were determined either via difference Fourier maps and refined with isotropic atomic displacement parameters or were calculated and fixed in ideal geometry, depending on data quality. The X-ray structures were analyzed and displayed using Mercury software.^[24] Crystallographic data have been deposited at the Cambridge Crystallographic Data Centre, CCDC: No CCDC 1501733 (**5c**), 1501734 (**5b**), 1501735 (**2a**), 1501736 (**2c**), 1501737 (**8a**) and 1501738 (**2b**). Copies of this information may be obtained free of charge from the Director, CCDC, 12 Union Road, Cambridge, CB2 1EZ, UK (+44-1223-336408; E-mail: deposit@ccdc.cam.ac.uk or <http://www.ccdc.cam.ac.uk>).

Molecular Modeling with NMR Constraints.

Three dimensional NMR structures of thienylpyridines were refined using the CHARMM program^[25] with potential function parameter set 22 from Discovery Studio.^[20] The Discovery Studio program was used to derive CHARMM force field parameters for the thienylpyridines applying MMFF partial charges. In simulations, we used only the force field derived by the Discovery Studio without the introduction of supplementary dihedral force field parameters based on our mechanic quantum simulations. During all CHARMM simulations, measured NOE (distance) restraints were applied with a force constant of 25 kcal/mol. Starting from the energy minimized structure, a dynamic simulation of 50 ns was carried out for each derivative at 300 K, with a time step of 1 fs. The dynamics were preceded

by heating (during 3 ps) and equilibration (25 ps) steps. During the production phase (50 ns), conformations were saved every 5 ps and energy minimized to a root-mean-square gradient of less than 0.001 kcal/(mol·Å²). The 10 lowest-energy conformations obtained for each thienylpyridyl compound were used in the subsequent analysis. The selected structures were analyzed and displayed using Mercury software.^[24]

Acknowledgements

The authors gratefully acknowledge the CRIHAN (Centre de Ressources Informatiques de Haute Normandie), as well as the European Community (FEDER) for the molecular modelling software.

Keywords: β -strand mimetic • foldamers • oligothiopyridines • NMR and X-ray studies • molecular modelling

- [1] O. Keskin, A. Gursay, B. Ma and R. Nussinov, *Chem. Rev.* **2008**, *108*, 1225–1244.
- [2] a) T. Clackson, J. A. Wells and *Science* **1995**, *267*, 383–386; b) G. Wenxing, J. A. Wisniewski and J. Haitao, *Biorganic & Medicinal Chemistry Letters* **2014**, *24*, 2546–2554.
- [3] M. R. Arkin and J. A. Wells, *Nat. Rev. Drug Discov.* **2004**, *3*, 301–317.
- [4] a) A. J. Wilson, *Progress in Biophysics and Molecular Biology* **2015**, *119*, 33–40; b) M. K. P. Jayatunga, S. Thompson and A. D. Hamilton, *Bioorganic & Medicinal Chemistry Letters* **2014**, *24*, 717–724; c) M. Lanning and S. Fletcher, *Biology* **2015**, *4*, 540–555.
- [5] H. Remaut and G. Waksman, *Trends Biochem Sci* **2006**, *31*, 436–444.
- [6] a) W. A. Loughlin, J. D. A. Tyndall, M. P. Glenn, T. A. Hill and D. P. Fairlie, **2010**, *Chem. Rev.*, PR32–PR69; b) A. G. Jamieson, D. Russell and A. D. Hamilton, *Chemical Communications* **2012**, *48*, 3709–3711; c) C. L. Sutherland, S. Thompson, R. T. W. Scott and A. D. Hamilton, *Chemical Communications* **2012**, *48*, 9834–9837; d) E. A. German, J. E. Ross, P. C. Knipe, M. F. Don, S. Thompson and A. D. Hamilton, *Angew. Chem. Int. Ed.* **2015**, *127*, 2687–2690; e) J. E. Ross, P. C. Knipe, S. Thompson and A. A. Hamilton, *Chem. Eur. J.* **2015**, *21*, 13518–13521; f) L. Sebaoun, V. Maurizot, T. Granier, B. Kauffmann and I. Huc, *J. Am. Chem. Soc.* **2014**, *136*, 2168–2174.
- [7] A. B. Smith III, T. P. Keenan, R. C. Holcomb, P. A. Sprengeler, M. C. Guzman, J. L. Wood, P. J. Carroll and R. Hirschmann, *J. Am. Chem. Soc.* **1992**, *114*, 10672–10674.
- [8] P. N. Wyrembak and A. D. Hamilton, *J. Am. Chem. Soc.* **2009**, *131*, 4566–4567.
- [9] a) A.-S. Voisin, A. Bouillon, G. Burzicki, M. Célan, R. Legay, H. El-Kashef and S. Rault, *Tetrahedron* **2009**, *65*, 607–612; b) G. Burzicki, A.-S. Voisin-Chiret, J. Sopkova-de Oliveira Santos and S. Rault, *Tetrahedron* **2009**, *65*, 5413–5417; c) G. Burzicki, A.-S. Voisin-Chiret, J. Sopkova-de Oliveira Santos and S. Rault, *Synthesis* **2010**, *16*, 2804–2810; d) A.-S. Voisin-Chiret, M. Muraglia, G. Burzicki, S. Perato, F. Corbo, J. Sopkova-de Oliveira Santos, C. Franchini and S. Rault, *Tetrahedron* **2010**, *66*, 8000–8005; e) S. Perato, A.-S. Voisin-Chiret, J. Sopkova-de Oliveira Santos, M. Sebban, R. Legay, H. Oulyadi and S. Rault, *Tetrahedron* **2012**, *68*, 1910–1917; f) M. De Giorgi, A.-S. Voisin-Chiret, J. Sopkova-de Oliveira Santos, F. Corbo, C. Franchini and S. Rault, *Tetrahedron* **2011**, *67*, 6145–6154.
- [10] J. Sopkova-de Oliveira Santos, A.-S. Voisin-Chiret, G. Burzicki, L. Sebaoun, M. Sebban, J.-F. Lohier, R. Legay, H. Oulyadi, R. Bureau and S. Rault, *J. Chem. Inf. Model.* **2012**, *52*, 429–439.
- [11] S. Perato, J. Fogha, M. Sebban, A.-S. Voisin-Chiret, J. Sopkova-de Oliveira Santos, H. Oulyadi and S. Rault, *Journal of Chemical Information and Modeling* **2013**, *53*, 2671–2680.

- [12] B. R. Beno, K.-S. Yeung, M. D. Bartberger, L. D. Pennington and N. A. Meanwell, *J. Med. Chem.* **2015**, *58*, 4383-4438.
- [13] H. Peacock, J. Luo, T. Yamashita, J. Luccarelli, S. Thompson and A. D. Hamilton, *Chemical Science* **2016**, *Advance Article*. doi:10.1039/C6SC00756B
- [14] Y. Che, B. R. Brooks and G. R. Marshall, *J. Comput. Aided Mol. Des.* **2006**, *20*, 109-130.
- [15] E. Jacoby, *Biorg. Med. Chem. Lett* **2002**, *12*, 891-893.
- [16] a) A. Bouillon, J.-C. Lancelot, V. Collot, P.-R. Bovy and S. Rault, *Tetrahedron* **2002**, *58*, 2885-2890; b) A. Bouillon, J.-C. Lancelot, V. Collot, P.-R. Bovy and S. Rault, *Tetrahedron* **2002**, *58*, 3323-3328; c) A. Bouillon, J.-C. Lancelot, V. Collot, P.-R. Bovy and S. Rault, *Tetrahedron* **2002**, *58*, 4369-4373; d) A. Bouillon, J.-C. Lancelot, J. Sopkova-de Oliveira Santos, V. Collot, P.-R. Bovy and S. Rault, *Tetrahedron* **2003**, *59*, 10043-10049.
- [17] a) A. S. Voisin, A. Bouillon, I. Berenguer, J.-C. Lancelot, A. Lesnard and S. Rault, *Tetrahedron* **2006**, *62*, 11734-11739; b) T. Cailly, F. Fabis, A. Bouillon, S. Lemaitre, J. Sopkova-de Oliveira Santos and S. Rault, *Synlett* **2006**, *1*, 53-56.
- [18] D. Neuhaus and M. P. Williamson, *The Nuclear Overhauser Effect in Structural and Conformational Analysis*, Inc.: New York, **2000**, p.
- [19] C. R. Jones, C. P. Butts and J. N. Harvey, *Beilstein J. Org. Chem.* **2011**, *7*, 145-150.
- [20] in *Discovery Studio Modeling Environment*, release 3.5, Vol. (Ed. A. S. Inc.), San Diego, CA, **2012**.
- [21] M. J. Frish, G. W. Trucks, H. B. Schlegel, G. E. Scuseria, M. A. Robb, C. J. R., J. Montgomery, J. A. , V. T., K. N. Kudin, J. C. Burant, J. M. Millam, S. S. Iyengar, J. Tomasi, V. Barone, B. Mennucci, M. Cossi, G. Scalmani, N. Rega, G. A. Petersson, H. Nakatsuji, M. Hada, M. Ehara, K. Toyota, R. Fukuda, J. Hasegawa, M. Ishida, T. Nakajima, Y. Honda, O. Kitao, H. Nakai, M. Klene, X. Li, J. E. Knox, H. P. Hratchian, J. B. Cross, V. Bakken, C. Adamo, J. Jaramillo, R. Gomperts, R. E. Stratmann, O. Yazyev, A. J. Austin, R. Cammi, C. Pomelli, J. W. Ochterski, P. Y. Ayala, K. Morokuma, G. A. Voth, P. Salvador, J. J. Dannenberg, V. G. Zakrzewski, S. Dapprich, A. D. Daniels, M. C. Strain, O. Farkas, D. K. Malick, A. D. Rabuck, K. Raghavachari, J. B. Foresman, J. V. Ortiz, Q. Cui, A. G. Baboul, S. Clifford, J. Cioslowski, B. B. Stefanov, G. Liu, A. Liashenko, P. Piskorz, I. Komaromi, R. L. Martin, D. J. Fox, T. Keith, M. A. Al-Laham, C. Y. Peng, A. Nanayakkara, M. Challacombe, P. M. W. Gill, B. Johnson, W. Chen, M. W. Wong, C. Gonzalez and J. A. Pople in *Gaussian Revision C.02*, Vol. (Ed. I. W. Gaussian 03, CT, 2004).
- [22] G. M. Sheldrick, *Acta Crystallogr.* **1990**, *A46*, 467-473.
- [23] G. M. Sheldrick, *Acta Crystallogr.* **2008**, *A64*, 112-122.
- [24] C. F. Macrae, P. R. Edgington, P. McCabe, E. Pidcock, G. P. Shields, R. Taylor, M. Towler and J. van de Streek, *J. Appl. Cryst.* **2006**, *39*, 453-457.
- [25] B. R. Brooks, R. E. Brucoleri, B. D. Olafson, D. J. States, S. Swaminathan and M. Karplus, *J. Comput. Chem.* **1983**, *4*, 187-217.

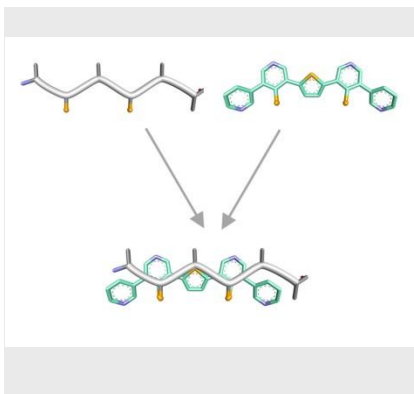
Entry for the Table of Contents (Please choose one layout)

Layout 1:

FULL PAPER

Protein-protein interactions (PPIs) are involved in many cellular processes and the design of small molecules as modulators of PPIs is an important challenge. Actually, the most challenging PPIs classes are those mediated by β -sheet interactions. This study reports the use of S...N interactions as a conformational control in oligothiienylpyridyl scaffolds in view of their ability for β -strand mimicry

Key Topic: Foldamer; β -strand



Marie Jouanne, Anne Sophie Voisin-Chiret,* Rémi Legay, Sébastien Coufourier, Sylvain Rault and Jana Sopkova-de Oliveira Santos*

Page No. – Page No.

Beta strand mimicry: Exploring oligothiienylpyridines foldamers

Accepted Manuscript